Waste thickness estimation at a large landfill in Brazil from a comparison of simultaneous inversion of different electrode arrays data set

Victória basileu de oliveira Lima
University of Brasília
Victor Cavalcanti Bezerra Guedes
University of Brasília
Mirella basileu de oliveira Lima (mirellabasileu@gmail.com)
Federal University of Paraná
Welitom Rodrigues Borges
University of Brasília
Luciano Soares da Cunha
University of Brasília

Research Article

Keywords: simultaneous inversion, Resistivity tomography, Landfill volume

Posted Date: April 5th, 2022

DOI: https://doi.org/10.21203/rs.3.rs-1511234/v1

Abstract

Electrical resistivity tomography (ERT) is particularly suitable for stratigraphic characterization of landfills given its sensitivity to the conductive response of leachate from solid waste. In this context, the simultaneous inversion of data from more than one electrode array can be more reliable than the single inversion of a single set of this data. In this way, resistivity lines were acquired in four electrode arrays at the Jockey Clube landfill in Brazil. We carried out the simultaneous inversion of all possible combinations of the Dipole-dipole (DD), Pole-dipole (PD), Wenner (WN) and Wenner-Shlumberger (WS) arrays and compared the results with direct information from 5 drill holes. The participation of the WN and WS electrode array data obtained similar results when grouped, and the WN and DD matrices, when inverted together, favored the horizontal resolution and the depth of investigation when compared with the inversion of the array separately. To estimate the depth of the waste layer, all available information was used to produce a geoelectric model based on the interpolation of approximate resistivity isovalues at the top and bottom of the waste landfill. The model points to a layer of waste that can vary from 30 to 65 meters in depth, and a total volume of 23,340,429 m³. Finally, the simultaneous inversion of arrays can be a useful tool for landfill investigation, especially if the geoelectric models of the matrices are quite different from each other, in which the subsurface structure is complicated with little a priori information.

Introduction

Municipal solid waste landfill (MSWL) are open deposition areas that were not planned in accordance with measures to protect the environment and public health. In these places, there is no control over the disposal of the discarded materials, nor a drainage system for the leachate generated from the waste composition (Hoornweg and Brada-tata 2012). The historical reconstruction of waste disposal for an MSWL is a challenging task. Geoelectric methods are a quick, non-invasive and detailed way to obtain estimates regarding the vertical and lateral extent of the waste package mass.

Electrical resistivity tomography (ERT) has been widely used for investigation in areas of urban solid waste deposition, from identifying contamination plumes (Loke and Dahlin 2002; Osella et al. 2002; Rosqvist et al. 2011; Clément et al. 2010; Lopes et al. 2012; Cavalcanti et al. 2014; Netto et al. 2020;) to the delimitation of the different strata of the landfill (Bernstone et al. 2000; Soupios et al. 2007; Aziz et al. 2019;). One way to improve the application of this technique is to mark out the interpretations of the ETR sessions with direct information, such as drillholes (Auken and Christiansen 2004; Wisén et al. 2005; Deceuster et al. 2006; Heincke et al. 2010; AL-Hameedawi and Thabit 2017; Aziz et al. 2019). In this way, it is possible to reduce ambiguities in the interpretation of images and to adjust the data processing routine in a real sphere of landfill investigation.

Several factors can influence the quality of measurements in an ERT survey, such as the quality of the equipment used, the quantity and spacing of the electrodes and the surface of the investigated medium (Loke 2011). The choice of electrode array is one of the most influential factors when it comes to subsurface image resolution (Martorana et al. 2009; Moreira et al. 2016) and there is a growing interest in

comparing the results obtained, especially when modeled separately and for combinations of different configurations (Dahlin and Zhou 2006; AL-Hameedawi and Thabit 2017; Eissa et al. 2019). In order to choose an ideal electrode configuration, some parameters must be considered, such as: 1) the depth of investigation; 2) the structure in which it is intended to investigate (vertical or horizontal); 3) the acquisition time; 4) the signal strength; and 5) the software available for processing and modeling the data. In practice, there is a trend towards the use of more traditional 2D imaging arrangements, such as the Wenner, Wenner-Schlumberger, Pole-pole, Pole-dipole and Dipole-dipole configurations (Loke 2011; Szalai and Szarka 2008).

There is controversy regarding the choice of the best electrode arrangements for the application of landfill studies. Dahlin and Zhou (2004) compared ten electrode arrays in five synthetic geological models in terms of resolution and signal-to-noise ratio. The authors recommended the Pole-dipole, dipole-dipole, Wenner-b and gradient arrangements for 2D imaging of ERT in landfills. However, Moreira et al. (2016) and AL-Hameedawi and Thabit (2017), affirm that the Dipole-Dipole configuration is not suitable for investigations of thick landfills due to the lower signal-to-noise ratio and the decrease in vertical resolution when there is an increase in depth. The authors remark that the data set obtained with the Wenner (WN) and Wenner-Schlumberger (WS) arrangements are a satisfactory alternative for the calculus of inverse models that best delineate the subsurface layers. In order to obtain an acceptable resolution and, at the same time, high speed of data acquisition, Martorana et al. (2017) state that the data set for the Dipole-Dipolo (DD) arrangement and high coverage gradient are more suitable.

Normally, the resistivity data obtained in the surveys generate good results for individual inversion for each type of commom arrangement. However, it is possible to obtain satisfactory results when data from different electrode arrays are concatenated in a simultaneou**s** inversion over the same location (Zhou and Greenhalgh 2000; Stummer et al. 2004; Athanasiou et al. 2007; Candansayar 2008; Konstantaki et al. 2015; Demirel and Candansayar 2016; Hermans and Paepen 2020). The use of the simultaneou**s** inversion technique can amplify the results by combining the relative advantages of each electrode array. De la Vega et al. (2003) and Konstantaki et al. (2015) used the results of the combined inversion of the dipole-dipole and Wenner arrangements to increase the depth of investigation in subsurface and to improve the resolution of the characteristics of the investigated substrate. The authors suggested that the simultaneou**s** inversion of WN-DD shows better lateral resolution when compared with the results of the inversions of each electrode array separately.

In this paper we present an experimental procedure to estimate which electrode configurations produced the best results regarding the stratigraphy of an old controlled landfill in Brasília, Brazil. Thus, the main objectives of the present work are: a) To compare the results obtained with those of different arrangements in all possible combinations of simultaneou**s** inversions for the Dipole-Dipole (DD), Pole-Dipole (PD), Wenner (WN) and Wenner-Schlumberger (WS) arrangements; b) To determine a thickness model and calculate the approximate volume of the solid waste package from the most representative geoelectric model of the landfill.

Study area

The Jockey Clube Controlled Landfill (ACJC) is located at about 20 km from the center of Brasilia, Brazil. The beginning of the deposition of waste at the ACJC took place in the late 1960s, and today, after having its activities officially closed in early 2018, the site functions only as a Rubble Receiving Unit (RRU) in the central part of the old landfill. The site is known as the largest open-air disposal area in Latin America (Fig.1a) (Campos et al. 2018).

In the initial years of operation of the landfill, Koide and Bernardes (1998) reported that the waste was disposed of in trenches using the ramp method, in which the soil removed from the excavation was used to cover the garbage trench. For many years, there has been no control of the drainage of surface and underground leachate, and no gas dispersing system. In some portions of the landfill, waste was disposed of completely randomly over natural soil. In the last decade of the ACJC's operation, some structural measures were carried out that allowed the site to be classified as a controlled landfill, and not as a dumping ground.

The geological context that makes up the framework of the study area are the rocks of the Paranoá Group, of Meso/Neoproterozoic age, more specifically the Formation Ribeirão do Torto. This unit is composed of slates. In this set, two penetrative foliations are observed that represent the slates' cleavages and configure the character of the friable and brittle rock. Associated with this lithotype, well-developed oxisol profiles (more than 20 m deep) overlaid with saprolites that correspond to highly weathered slates (Campos et al. 2013). The geotechnical characteristics point to a very homogeneous soil, with high porosity (> 60%) and permeability, and with a high content of the clay fraction (> 50%; Pastore et al., 1998).

The predominant relief in the study region is flat to slightly undulating hills, with slopes less than 10% and elevations greater than 1100 m. In the scope of the study area, the natural topography has been intensely modified since the beginning of the ACJC's operation.

Currently, the site has been modified in such a way that the center of the landfill is a topographic peak known informally as "Wedding cake". It is known that the ACJC landfill is stratigraphically subdivided into 4 layers: construction waste (CCW), solid waste, oxisol, and solid rock (slate).

Materials And Method

Data acquisition

The technique used in the investigation of the ACJC was the Electrical Resistivity Tomography (ERT). Four profiles were acquired in 2019 (L1 to L4), each measuring 710 meters, in the portion known as “Wedding cake” (Fig. 1b). Four different electrode arrays were used: WN, WS, DD, PD.

Direct information from three Reverse circulation drillholes (Pastore et al. 1998) and two drillholes in 2020 (PG1 and PG2), were used to contribute to the interpretation of the resistivity models. The resistivity

data was not acquired precisely from the drillholes, due to the intense traffic of trucks and machines from the daily activities of the landfill, or because they are now in embargoed areas with difficult access or dense vegetation. It is assumed, for the purpose of correlating direct and indirect information, that there is no strong variation in the geometry of the top of the rock substrate, therefore it is possible to correlate the information of the drillholes directly to the ERT lines.

The acquisition system used was the Syscal Pro (IRIS Instruments) and the sequences for each electrode array were configured before data acquisition by the Electre II software (Iris instruments). The Acquisition parameters for each electrode configuration Dipole-Dipole (DD), Polo-Dipole (PD), Wenner (WN), Wenner-Schlumberger (WS) was 72 amount of steel electrodes (73 for PD), 710 m line length, 400 Vab of voltage, 250 ms of infection time.

After the field acquisition, the data was stored in the equipment's memory and transferred to the Prosys III software (IRIS Instruments), where the data was filtered. The resulting apparent resistivity values that were greater than twice the standard deviation were removed during the filtering process, as were some of the outliers.

Modeling resistivity data

The filtered data was exported to the Res2DInv software. The robust inversion methods, or L1-norm (Loke et al. 2003) and inversion by least squares with smoothness restriction, or L2-norm (Loke and Dahlin 2002), were used for comparison in Guedes et al. (2020), where the robust inversion made anomalies smoother in shape, since the spurious points have less weight in the modeling process, and generated models with more horizontal features that more satisfactorily delimit the waste package base. Therefore, the robust inversion was chosen for the present work.

From the apparent resistivity values obtained in each electrode configuration, 2D simultaneou**s** inversion models of all possible combinations were elaborated for the four measurements of the acquired arrangements (WN, WS, DD, PD) of the four ERT lines, totaling 15 resistivity sections per line. For this purpose, inversion parameters of the vertical to horizontal leveling filter equal to 0.3 were used to highlight horizontal structures, and a grid size model equal to the actual spacing between the electrodes.

Model validation and numerical simulation

After obtaining the ETR's, the best combinations of electrodes arrangements were selected according to the resistivity values related to the ACJC's historical context. The selection criterion for the best session was performed by analyzing the behavior of the resistivity value of the ETR for each array combination at the location where we obtained direct information from the 4 drillholes. The variation of the resistivity values of 5 meters above and below the limits between Civil Construction Waste (CCW) and waste (top of the waste package), and the limit between waste and the oxisol (waste package base) were analyzed. Within these limits, the difference between the last element of this set and the first, known as Range, was calculated. This parameter provides a measure of the dispersion of the values, but not of how they are

distributed. For this reason, an analysis of linear regression using the ordinary least squares (OLS) method was performed for each set of resistivity values in the top and bottom intervals of the waste package (x) as a function of depth (μy) (Gujarati and Porter 2011; Sheard 2018), according to the model:

$$\mu_y = \beta_0 + \beta_1$$

Where $\beta 1$ is the regression coefficient, which expresses the slope of the line or the shape. The greater the contrast of resistivity at the top and bottom limits of the waste package, that is, the lower the value of $\beta 1$ at the limit of CCW and waste, and the greater the value of $\beta 1$ at the limit of Waste and soil regarding the resistivity of the models, more coherent the ETR is with the ACJC's historical deposition context.

The values of Range and $\beta 1$ for each profile analyzed were grouped in a table and from those, a ranking of the session was drawn up that best defines the limits of CCW, Waste and soil. To choose the session that is most consistent with the ACJC context, the following were also considered: 1) lowest absolute error between the observed and calculated model; 2) the depth of investigation achieved; 3) correspondence with the drillholes; and 4) the representativeness of the model in relation to the horizontality of the delimitation of the layers and the waste package base.

To validate the numerical performance of the statistical analysis of the resistivity profiles, a numerical modeling of the line 1 session was performed for all combinations of arrangements, and the range and $\beta 1$ were calculated to compare the same values with the line 1 session measured in the field. Fifteen theoretical models were used to evaluate the models in line 1. For the construction of the models, we used the information from the drillhole PG1. 3 hypothetical horizontal layers were considered. The superficial layer simulates the CCW, with resistivity for a layer of 100 Ω.m and 18 meters of depth. The second layer simulates the conditions of the waste layer, with an average resistivity of 20 Ω.m and 24 meters of thickness. Finally, the third layer simulates the geological substrate of the landfill, with an average resistivity of 200 Ω.m and 38 meters of thickness. The commercial software RES2DMOD (Barker 1996) was used to generate the models for comparison.

In all models, 72 electrodes with a spacing of 10 meters were used, simulating the real field acquisitions. Four electrode configurations (WN, WS, DD, PD) were used to generate the apparent resistivities of up to 30 levels. The data was concatenated and inverted in the res2Dinv program using the L1 standard inversion. To represent realistic field conditions, 5% noise was added to the apparent resistivity, before inversion. The inversion settings for the synthetic model data are the same as the settings used to invert the actual field data. The inverted sessions of the numerical model can be seen in Fig. 2. The absolute error varied between 4.13% and 5.17% for the 15 models.

Waste thickness model

After choosing the session that best fit the criteria, the elevation data for the resistivity isovalues for the base and the trend in the resistivity value for the top of the waste layer in the central portion of the landfill

were extracted for each image of the chosen combination.

The estimated grid dimension of the top and bottom of the waste layer was generated in the Surfer software (Golden software) by the ordinary kriging method with an exponential function for the semivariogram. The parameters of the theoretical function such as Sill and Range, as well as the anisotropy axes were adjusted and validated by the method of cross validation. To evaluate the quality of the grids, the analysis of the percentage error histogram was performed and to evaluate accuracy and precision, the root mean squared error (RMSE) and Pearson's correlation coefficient were calculated (φ).

The absolute difference between both surfaces made it possible to elaborate a model of the thickness of the layer of landfilled waste, as well as its approximate volume. The thickness model was limited to the region defined in Fig. 1. The topographic elevation referring to this limit was inserted as a priori information during the interpolation of the surface referring to the base of the waste layer, since the electroresistivity lines did not sample these edges properly. This was done to avoid erroneous extrapolations in the final model.

Results And Discussion

The results of the simultaneou**s** inversions can be seen in Fig. 3, 4, 5 and 6. In all sessions there is a predominance of low resistivity values, which suggests a strong influence of conductive materials in the composition of the landfill, probably associated with the leachate material from the decomposition of organic waste from the landfill.

All sessions have a large zone of low resistivity in the body of the landfill, between 5 to 50 Ω.m. This zone possibly corresponds to the waste package deposited over the years. Above this conductive zone, it is possible to observe, in the first meters of the sessions, an irregular layer of higher resistivity, between 40 to 180 Ω.m. The layer in question may correspond to the coverage of construction waste (CCW), deposited in more recent years of operation of the landfill. At higher depths, the sections have higher resistivity values in relation to the intermediate conductive portion of the landfill, between 100 and 200 Ω.m.

This can be associated with the natural geological substrate existing in the subsurface. The transition from low resistivity and higher resistivity values occurs gradually. The resistivity values calculated for the latosol in subsurface areas were much lower than the values expected for the latosol in the region (Cavalcanti et al., 2014; Seimetz et al., 2013). The reason for this fact may be related to the infiltration of the leachate material resulting from the decomposition of organic residues in the subsoil latosol.

When analyzing the images of the 4 arrays separately, Guedes et al. (2020) states that the DD arrangement is more coherent with the direct information extracted from the drillholes, and that the WN and WS arrangements highlighted the horizontal characteristic of the rock substrate in depth, although they do not correspond satisfactorily to the ground level in most of the lines. In the same paper, the

authors point out that the PD sessions had the least correspondence with the information obtained from the drillholes.

The L1 sessions were correlated with the drill holes PG1, PG2, SP-04 at 2, 10 and 30 meters of distance between the line, respectively, and can be seen in Fig. 3. By correlating the resistivity values and the information through the holes, the most representative model of the landfill, which best defines the base of the waste package and that possesses the least absolute error, is the model generated by the simultaneous inversion WN-WS-DD, which in turn has a value of approximately 30 Ω.m to the base of the waste package.

In view of the low correspondence of the models after inversion with the PD arrangement with the expected configuration of the landfill subsurface, when observing the L1 simultaneous inversions, it is possible to notice that the images obtained with the simultaneou inversion that present data from the PD arrangement also had little correspondence with the drillhole information. The models obtained with the WN and WS arrangements together did not show major differences.

The L2 sessions (Fig. 4) were not correlated with any of the holes, due to the long distance between them. The sessions that most resemble the structural configuration of the landfill, that is, three striking horizontal layers, were the inversions with data from DD-PD. However, the absolute error associated with the model was greater in relation to the measurements of the other inversions.

The L3 sessions were correlated with the SP-07 drillhole, approximately 75 meters away from the line, and can be seen in Fig. 5. When correlating the resistivity values and the direct information of the holes, the image generated by the arrangement DD obtained the least correspondence with the base of the waste package, while the WN and WS arrangements show the greatest similarity. However, when performing the simultaneous inversion of the arrangements, the model generated by the simultaneous inversion WN-DD and WN-DD-PD presented itself as the most coherent, due to the correspondence with the drillhole and greater lateral investigation of the surface of the base of the waste package. The approximate apparent resistivity value for the waste package base is of 40 Ω.m.

The L4 sessions were correlated with the SP-07 drillhole, about 150 meters from the line, and can be seen in Fig. 6. The models generated by the DD, WN and WS arrays tend to tilt to the most resistive layer, and the base of the waste package, according to the direct information of the drillhole, points to lower values of resistivity (approximately 10 Ω.m). When these arrays are concatenated with each other, the slope pattern of the resistive layer and the value of resistivities in general are maintained. In contrast, the sessions after inversion with data from the PD arrangement predominate the pattern of more horizontal layers and higher resistivity values for the waste package base (above 150 Ω.m).

Comparison and validation of models

After analyzing the resistivity profiles of the ETR along the positioning of the drillholes, it was possible to observe the numerical behavior of the variation of the resistivity values in depth. In addition, for each

multiple array, the resistivity contrast in the intervals of 5 meters above and below the CCW and Waste package (top of the waste package), and waste and soil (bottom of the waste package) were analyzed. The resistivity profiles of the resistivity model and the numerical model can be seen in Fig. 7.

Through statistical analysis, a ranking of the arrays combined with the best values of $\beta 1$ and Range was created for all resistivity profiles. The combination of WN-PD, WN-DD-PD, DD-PD arrays obtained the best results, respectively (Fig. 7b). When observing the resistivity sessions of the WN-PD configuration as a whole and not just where the drillhole is located, it is possible to state that the sessions present the expected horizontality for the landfill layers, and the depth of investigation achieved by combining the WN-DD arrangement was greater in relation to the WN and DD arrangements separately. The absolute error between the observed model and the ETR decreased in relation to the DD arrangement, however, it remains one of the combinations of the arrangement with the most errors. Despite this, the images of the simultaneous inversion of WN-DD were chosen to generate the thickness model of the ACJC residue layer, considering the several positive factors that point out the combination of the WN-DD arrangement as adequate.

According to the ranking of the resistivity profile of the numerical analysis, the WN-DD, WN-DD-PD configurations also obtained the greatest variations in the waste package limits, which reaffirms the choice of the WN-DD arrangement for the elaboration of the waste thickness model, and validates the statistical analysis previously performed.

Waste thickness model

In Line 1, the approximate resistivity value used to extract the elevation from the base of the waste layer was 30 Ω.m. In L3 and L4, the surface of approximate values corresponded to 20 and 10 Ω.m, respectively. Bearing in mind that L2 does not present direct drillhole information, the values extracted from the profile correspond to the average of the resistivity values extracted from the other lines (20 Ω.m). The elevation values for the top of the waste package were extracted from the resistivity contrast in the initial meters of the sessions and based on direct information from PG1 and PG2. The lines of approximate resistivity values used for interpolation of the base and top of the waste package can be seen in Fig. 8a.

The interpolated model of the waste thickness has a greater thickness in the center of the waste package and decreases towards the limits of the investigated area. The layer of landfilled waste can reach up to a depth of 65 meters. In addition, it is estimated that the approximate volume of landfilled waste is approximately 23,340,429 m³, based on the cubic model generated.

The percentage error histogram of the top and bottom grids of the generated model is relatively symmetrical with a percentage average of approximately 0 and with little dispersion of the values, which points to the accuracy and precision of the interpolated grids. The statistical characteristics of Pearson's coefficient and RMSE for the grids have values close to 1 and 3 meters respectively, which indicates a strong direct correlation between the real and estimated values of the models, and a good accuracy of the

estimated results. The thickness model of the waste layer, as well as the statistical characteristics of parameterization and validation of the interpolation of the top and bottom of the layer, can be seen in Fig. 8.

Conclusions

In this present paper, the comparison of ETR models after individual and simultaneous inversion of acquired data with the Wenner, Wenner-Schlumberger, Dipole-dipole and Polo-dipole arrangements was discussed. The quotas referring to drillhole information were used to corroborate the interpretation of the sections and the evaluation of the results.

All sessions had a large zone of low resistivity, from 30 to 70 meters in the longitudinal direction, possibly associated with the area saturated by leachate. The delimitation of this zone can be established by the resistivity contrasts at the top and bottom of the ERT images, and the drillhole information. It is possible that the low resistivity values related to oxisol in this study are due to the flow of the contaminant in the subsurface, in view of the expected resistivity background for this soil in the region.

In all inversions with the WN and WS and arrangements it was possible to reach greater depths of investigation, however, the level of the most resistive layer associated with the soil was greater than the expected value, according to the drillhole data. In addition, the concatenation of WN and WS data did not return significant differences in the models.

The models generated by the PD configuration pointed out as the most divergent in relation to the direct information of the drillholes. When the data from this arrangement was concatenated with data from the WN, WS and DD configurations, differences were also observed in the combined inversions. One way to minimize the differences between the sessions and the direct information would be to include a weighting factor in the inversion, in order to partially balance the participation of the PD generation model arrangement.

From the comparative analysis carried out and the conclusions of Guedes et al. (2020), as for the recommendation of the dipole-dipole arrangement for investigations in the area, the simultaneous inversions of data WN and DD presented a new and efficient alternative. The ETR produced with the simultaneous inversion of the data of these two configurations was chosen as the most attractive option for interpretation, due to a good convergence with the dimensions obtained by the direct information, sufficient lateral resolution to characterize the extension of the base and top of the waste package, greater depth of investigation and acceptable mismatching errors between observed and calculated resistivity.

The extra time to acquire a large quantity of measurements for different arrangements can be a limitation. However, acquiring data on site with different electrode arrangements for carrying out simultaneous inversion routines is an option to be considered to expand the possibilities of data analysis and interpretation.

In order to refine the 3D model of the volume of solid waste obtained by the interpolation of the electrical imaging sessions, we recommended further electroresistivity acquisitions to better detail the subsurface of the ACJC, is that include transverse and longitudinal sections that intersect by entire area of investigation. Also, test other electrode arrays such as Pole-Dipole and Multiple Gradient. In this sense, we advisable to include in the field campaign other methods established in the literature for investigations of sanitary landfills, such as Induced Polarization in the Time Domain (Zonge et al., 2005; Donno and Cardarelli, 2017; Frid and Israel, 2017) due to the strong effect of Induced Polarization associated with the mass of solid waste.

Abbreviations

MSWL, Municipal solid waste landfill; DD, Dipole-dipole; PD, Pole-dipole; WN, Wenner; WS, Wenner-Shlumberger; ERT, Electrical resistivity tomography; ACJC, Jockey Clube Controlled Landfill; OLS, ordinary least squares; CCW, Civil Construction Waste;

Declarations

Acknowledgements

This study was financed in part by the Coordenação de Aperfeiçoamento de Pessoal de Nível Superior - Brasil (CAPES) - Finance Code 001. The authors are thankful to the RAEESA Project (University of Brasília/CEB Generation S.A. and CEB Lajeado S.A.) and the CAPES.

References

1. AL-Hameedawi MM, Thabit JM (2017) Comparison between four electrode arrays in delineating sedimentary layers of alluvial fan deposits in eastern Iraq using a 2D imaging technique. Environ. Earth Sci. 761:525. https://doi.org/10.1007/s12665-017-6853-9
2. Athanasiou EN, Tsourlos PI, Papazachos CB, Tsokas GN (2007) Combined weighted inversion of electrical resistivity data arising from different array types. Appl. Geophys. 62:124–140. https://doi.org/10.1016/j.jappgeo.2006.09.003
3. Auken E, Christiansen AV (2004) Layered e laterally constrained 2D inversion of resistivity data. Geophysics 69:752–761. https://doi.org/10.1190/1.1759461
4. Aziz NA, Abdulrazzaq ZT, Agbasi OE (2019) Mapping of subsurface contamination zone using 3D electrical resistivity imaging in Hilla city, Iraq. Environ. Earth Sci. 78:502. https://doi.org/10.1007/s12665-019-8520-9
5. Barker RD (1996) Practical techniques for 3D resistivity surveys e data inversionl, pp 499–523.
6. Bernstone C, Dahlin T, Ohlsson T, Hogland W (2000) DC-resistivity mapping of internal landfill structures: Two pre-excavation surveys. Environ. Geol. 39:360–371. https://doi.org/10.1007/s002540050015

7. Campos HKT (2018) Como fechamos o segundo maior lixão do mundo. Rev. Bras. Planej. e orçamento 8:204–253.
8. Campos JEG, Dardenne MA, Freitas-Silva FH, Martins-ferreira MAC (2013) Geologia do Grupo Paranoá na porção externa da Faixa Brasília. Brazilian J. Geol. 43:461–476. https://doi.org/10.5327/Z2317-48892013000300004
9. Candansayar ME (2008) Two-dimensional individual and joint inversion of three- and four-electrode array dc resistivity data *. J. Geophys. Eng. 5:290–300. https://doi.org/10.1088/1742-2132/5/3/005
10. Cavalcanti MM, Borges WR, Reiner S, Rocha MP, Cunha LS, Seimetz EX, Pedro V, Oliveira e Sousa, FRR de O (2014) Levantamento geofísico (eletrorresistividade) nos limites do Aterro Controlado do Jokey Clube, Vila Estrutural, Brasília - DF. Geociências (São Paulo) 33, 298–313.
11. Clément R, Descloitres M, Günther T, Oxarango L, Morra C, Laurent JP, Gourc JP (2010) Improvement of electrical resistivity tomography for leachate injection monitoring. Waste Manag. 30:452–464. https://doi.org/10.1016/j.wasman.2009.10.002
12. Dahlin T, Zhou B (2006) Multiple-gradient array measurements for multichannel 2D resistivity imaging. Near Surf. Geophys. 4:113–123. https://doi.org/10.3997/1873-0604.2005037
13. Dahlin T, Zhou B (2004) A numerical comparison of 2D resistivity imaging with 10 electrode arrays. Geophys. Prospect. 52:379–398. https://doi.org/https://doi.org/10.1111/j.1365-2478.2004.00423.x
14. De la Vega M, Osella A, Lascano E (2003) Joint inversion of Wenner and dipole – dipole data to study a gasoline-contaminated soil. J. Appl. Geophys. 54:97–109. https://doi.org/10.1016/j.jappgeo.2003.08.020
15. Deceuster J, Delgranche J, Kaufmann O (2006) 2D cross-borehole resistivity tomographies below foundations as a tool to design proper remedial actions in covered karst. J. Appl. Geophys. 60:68–86. https://doi.org/10.1016/j.jappgeo.2005.12.005
16. Demirel C, Candansayar ME (2016) Two-dimensional joint inversions of cross-hole resistivity data and resolution analysis of combined arrays. Geophys. Prospect. 65:876–890. https://doi.org/10.1111/1365-2478.12432
17. Donno G, Cardarelli, E, (2017) Tomographic inversion of time-domain resistivity and chargeability data for the investigation of landfills using a priori information. Waste Manag. 59, 302–315. https://doi.org/10.1016/j.wasman.2016.11.020
18. Eissa R, Cassidy N, Pringle, J, Stimpson, I (2019). Electrical resistivity tomography array comparisons to detect cleared-wall foundations in brownfield sites. Q. J. Eng. Geol. Hydrogeol. 53, 137–144. https://doi.org/10.1144/qjegh2018-192
19. Frid V, Israel N (2017). Leachate detection via statistical analysis of electrical resistivity and induced polarization data at a waste disposal site. Environ. Earth Sci. 76, 1–18. https://doi.org/10.1007/s12665-017-6554-4
20. Guedes VCB, Lima VB. de O, Borges WR, Cunha LS (2020) Comparison of the geoelectric signature with different electrode arrays at the Jockey Club landfill of Brasília. Brazilian J. Geophys. 38:1–12. https://doi.org/http://dx.doi.org/10.22564/rbgf.v38i1.2034

21. Gujarati DN, Porter DC (2011). Econometria Básica, 5th ed.
22. Heincke B, Günther T, Dalsegg E, Rønning JS, Ganerød GV, Elvebakk H (2010) Combined three-dimensional electric and seismic tomography study on the Åknes rockslide in western Norway. J. Appl. Geophys. 70:292–306. https://doi.org/10.1016/j.jappgeo.2009.12.004
23. Hermans T, Paepen M (2020) Combined inversion of land and marine electrical resistivity tomography for submarine groundwater discharge and saltwater intrusion characterization. Geophys. Res. Lett. 47:1–22. https://doi.org/10.1029/2019GL085877
24. Hoornweg D, Brada-tata P (2012) What a waste?: a global review of solid waste management., 15th ed. Washington.
25. Koide S, Bernardes RS (1998) Contaminação do lençol freático sob a a área do Aterro do Jockey Club, Distrito Federal., in: X Brazilian Congress of Groundwater. Federal District,. pp. 1–11.
26. Konstantaki LA, Ghose R, Draganov D, Diaferia G, Heimovaara T (2015) Characterization of a heterogeneous landfill using seismic and electrical resistivity data. Geophysics 80:13–25. https://doi.org/10.1190/geo2014-0263.1
27. Loke MH (2011) Tutorial : 2-D and 3-D electrical imaging surveys By.
28. Loke MH, Acworth I, Dahlin T (2003) A comparison of smooth and blocky inversion methods in 2D electrical imaging surveys. Explor. Geophys. 34:182–187. https://doi.org/https://doi.org/10.1071/EG03182
29. Loke MH, Dahlin T (2002) A comparison of the Gauss – Newton and quasi-Newton methods in resistivity imaging inversion. J. Appl. Geophys. 49:149–162. https://doi.org/10.1016/S0926-9851(01)00106-9
30. Lopes DD, Silva SMC, Fernandes F, Teixeira RS, Celligoi A, Dall'antônia luiz H (2012) Geophysical technique and groundwater monitoring to detect leachate contamination in the surrounding area of a landfill–Londrina (PR–Brazil). Environ. Manage. 113, 481–487. https://doi.org/https://doi.org/10.1016/j.jenvman.2012.05.028
31. Martorana R, Capizzi P, D'Alessandro A, Luzio D (2017) Comparison of different sets of array configurations for multichannel 2D ERT acquisition. J. Appl. Geophys. 137:34–48. https://doi.org/10.1016/j.jappgeo.2016.12.012
32. Martorana R, Fiandaca G, Ponsati AC, Consentino PL (2009) Comparative tests on different multi-electrode arrays using models in near-surface geophysics. J. Geophys. Eng. 6:1–20. https://doi.org/10.1088/1742-2132/6/1/001
33. Moreira CA, Lapola MM, Carrara A (2016) Comparative analyzes among electrical resistivity tomography arrays in the characterization of flow structure in free aquifer. Geofis. Int. 55:119–129. https://doi.org/10.22201/igeof.00167169p.2016.55.2.1716
34. Netto LG, Barbosa AM, Galli VL, Pereira JPS, Gandolfo OCB, Birelli CA (2020) Application of invasive and non-invasive methods of geo-environmental investigation for determination of the contamination behavior by organic compounds. J. Appl. Geophys. https://doi.org/https://doi.org/10.1016/j.jappgeo.2020.104049

35. Osella A, De La Vega M, Lascano E (2002) Characterization of a Contaminant Plume Due to a Hydrocarbon Spill Using Geoelectrical Methods. J. Environ. Eng. Geophys. 7:78–87. https://doi.org/https://doi.org/10.4133/JEEG7.2.78
36. Pastore EL, Souza NM, Pereira JHF, Franco HA et al (1998) Métodos de Investigação e Modelo Geológico–Geotécnico do Aterro de Lixo do Jóquei-Brasília/DF. XI Congr. Bras. Mecânica dos Solos e Eng. Geotécnica 3.
37. Rosqvist H, Leroux V, Dahlin T, Svensson M, Lindsjö M, Månsson CH, Johansson S (2011) Mapping landfill gas migration using resistivity monitoring. Proc. Inst. Civ. Eng. Waste Resour. Manag. 164: 3–15. https://doi.org/10.1680/warm.2011.164.1.3
38. Seimetz EX, Rocha MP, Borges WR, Nogueira PV, Cavalcanti MM, Azevedo PA (2013) Integration of geophysical methods to define the geological interfaces for a future metro station located in Brasilia - DF, Brazil. Geociencias 32:650–658.
39. Sheard J (2018) Quantitative data analysis, 2nd ed. Elsevier. https://doi.org/doi.org/10.1016/B978-0-08-102220-7.00018-2
40. Soupios P, Papadopoulos N, Papadopoulos I, Kouli M, Vallianatos F, Sarris A, Manios T (2007) Application of integrated methods in mapping waste disposal areas. Environ. Geol. 53:661–675. https://doi.org/10.1007/s00254-007-0681-2
41. Stummer P, Maurer H, Green AG (2004) Experimental design : Electrical resistivity data sets that provide optimum subsurface information. J. Appl. Geophys. 69:120–139. https://doi.org/https://doi.org/10.1190/1.1649381
42. Szalai S, Szarka L (2008) On the classification of surface geoelectric arrays. Geophys. Prospect. 56:159–175. https://doi.org/10.1111/j.1365-2478.2007.00673.x
43. Wisén R, Auken E, Dahlin T (2005) Combination of 1D laterally constrained inversion and 2D smooth inversion of resistivity data with a priori data from boreholes. Near Surf. Geophys. 3:71–79. https://doi.org/10.3997/1873-0604.2005002
44. Zhou B, Greenhalgh SA (2000) Cross-hole resistivity tomography using different electrode configurations. Geophys. Prospect. 48, 887–912. https://doi.org/10.1046/j.1365-2478.2000.00220.x
45. Zonge K, Wynn J, Urquhart S (2005) Resistivity, induced polarization, and complex resistivity. Near-surface Geophys. 265–300.

Figures

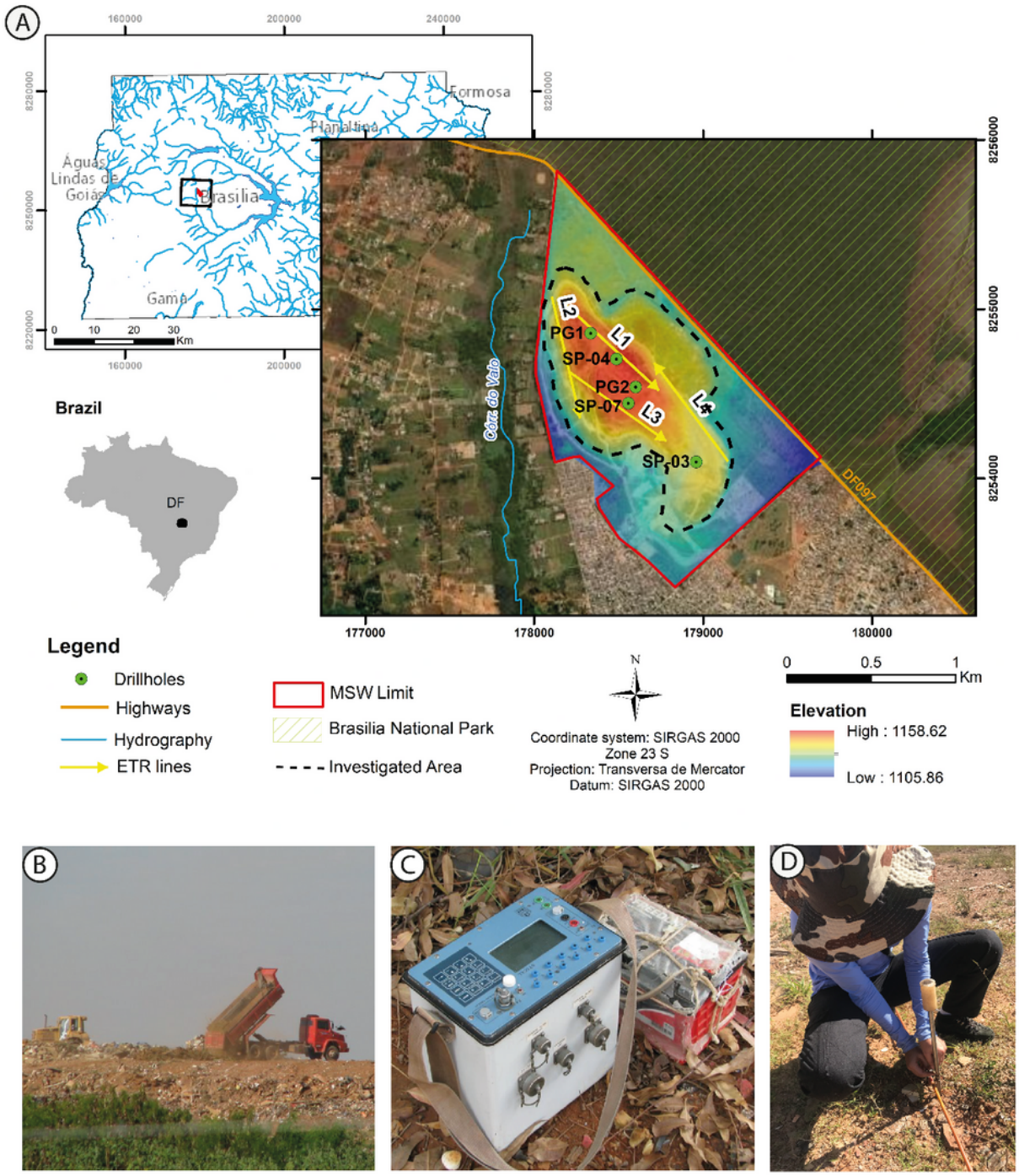

Figure 1

ACJC data acquisition. a) Location map of the L1 to L4 ERT lines, and the drillholes SP-04, SP-03 and SP-07 (1997), and PG1 and PG2 (2020). b) Present time image of the area known as 'wedding cake', while in operation. c) The acquisition system used "Syscal Pro". d) Multi-eletrode sunked into the ground for data acquisition.

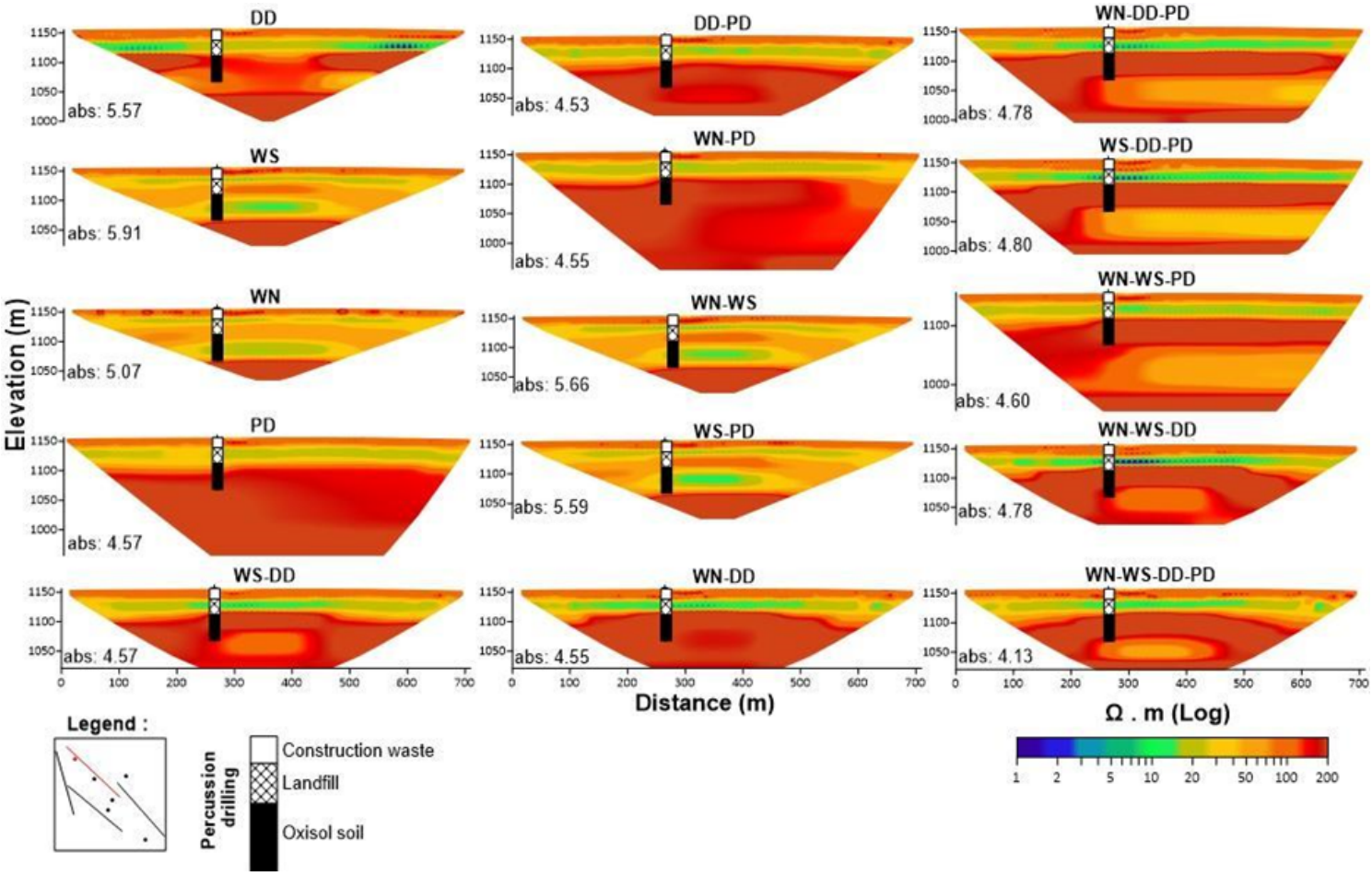

Figure 2

Numerical models from session 1 for 15 multiple arrays. Simulation carried out from the historical reconstruction of the ACJC and the direct information from drillhole PG1.

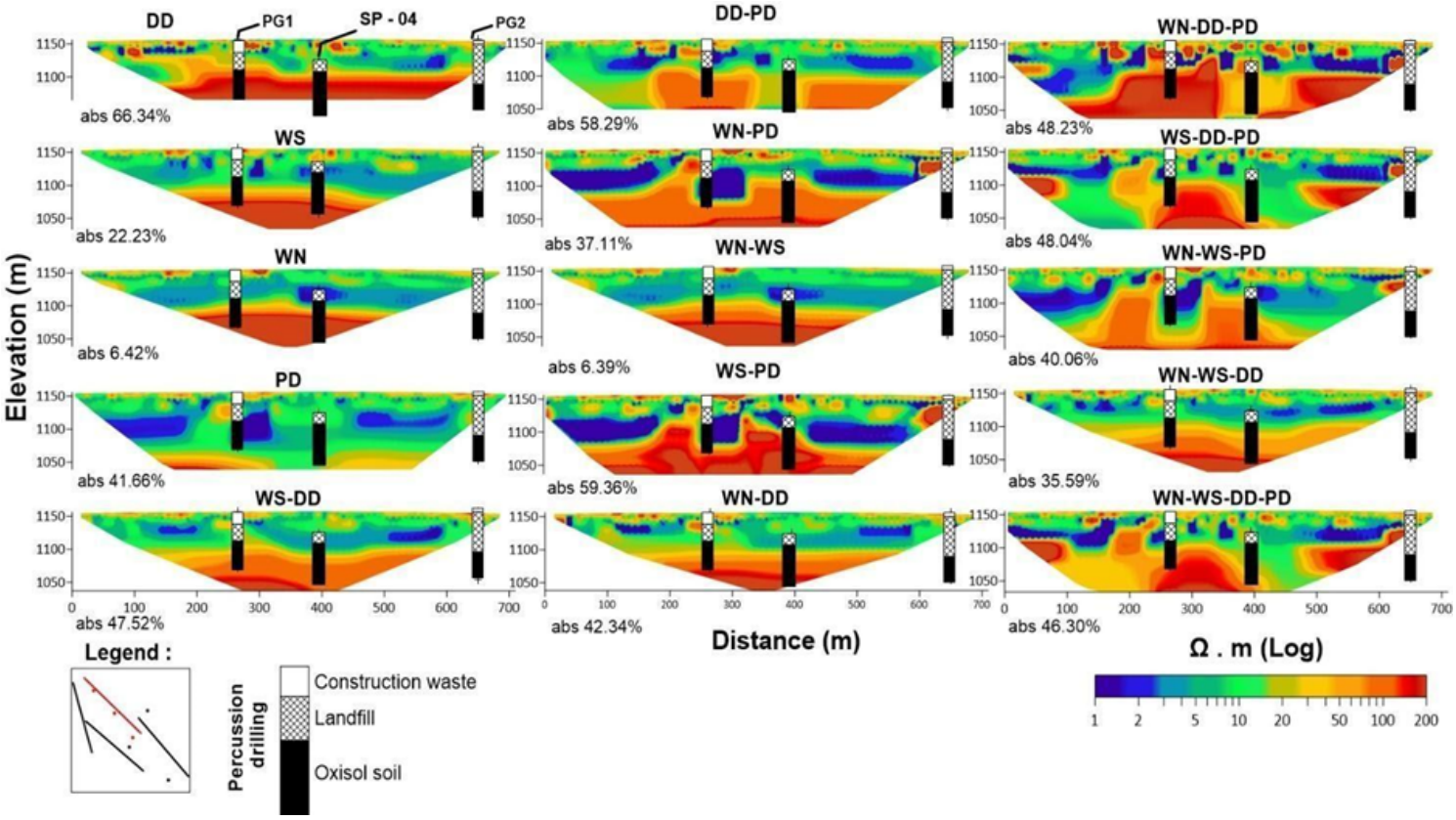

Figure 3

Comparison between resistivity sessions for line 1 obtained for the 4 arrays and 11 inversion combinations, associated with the drillholes PG1, PG2 and SP-04.

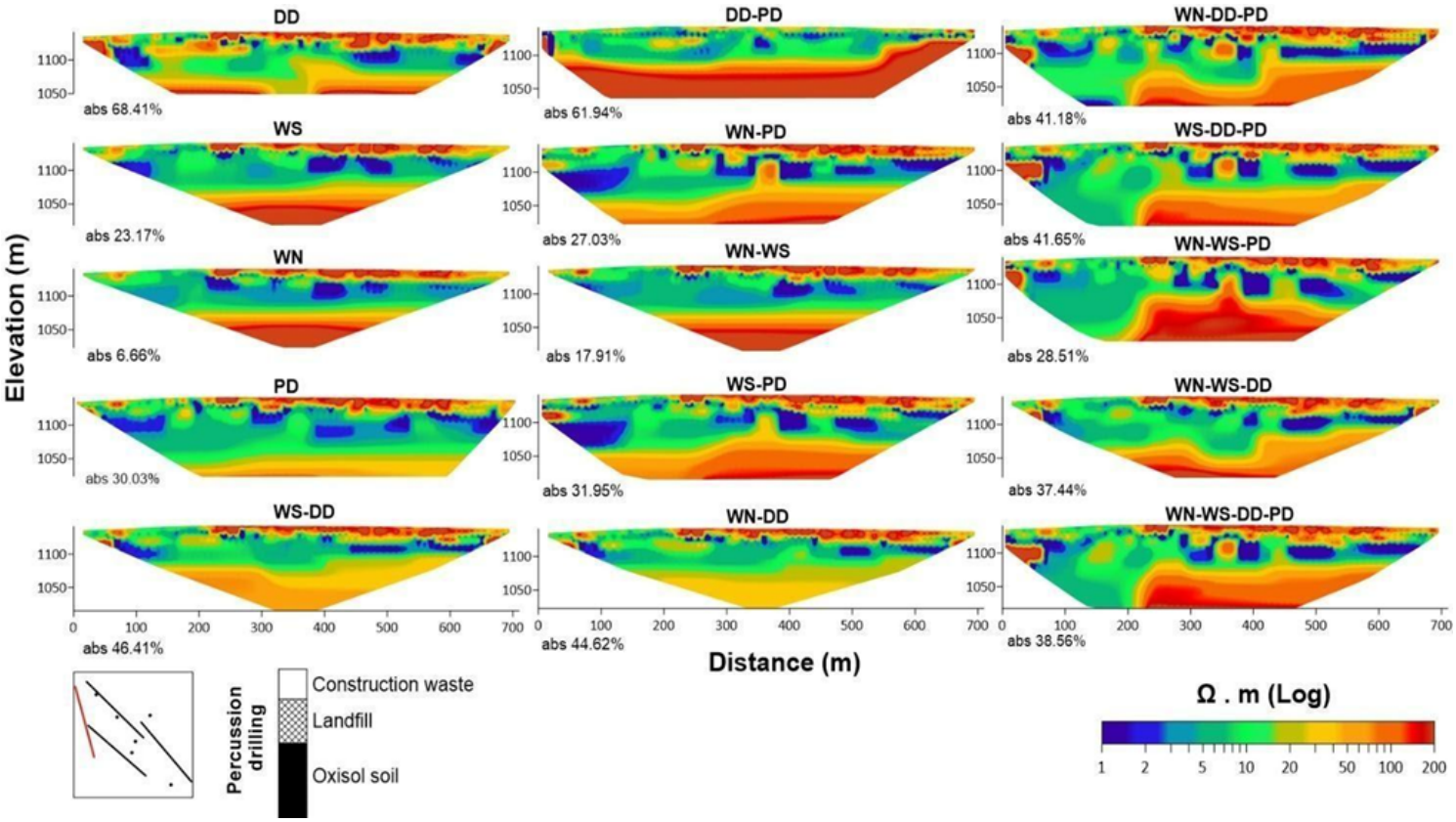

Figure 4

Comparison between resistivity sessions for line 2 obtained for the 4 arrays and 11 inversion combinations.

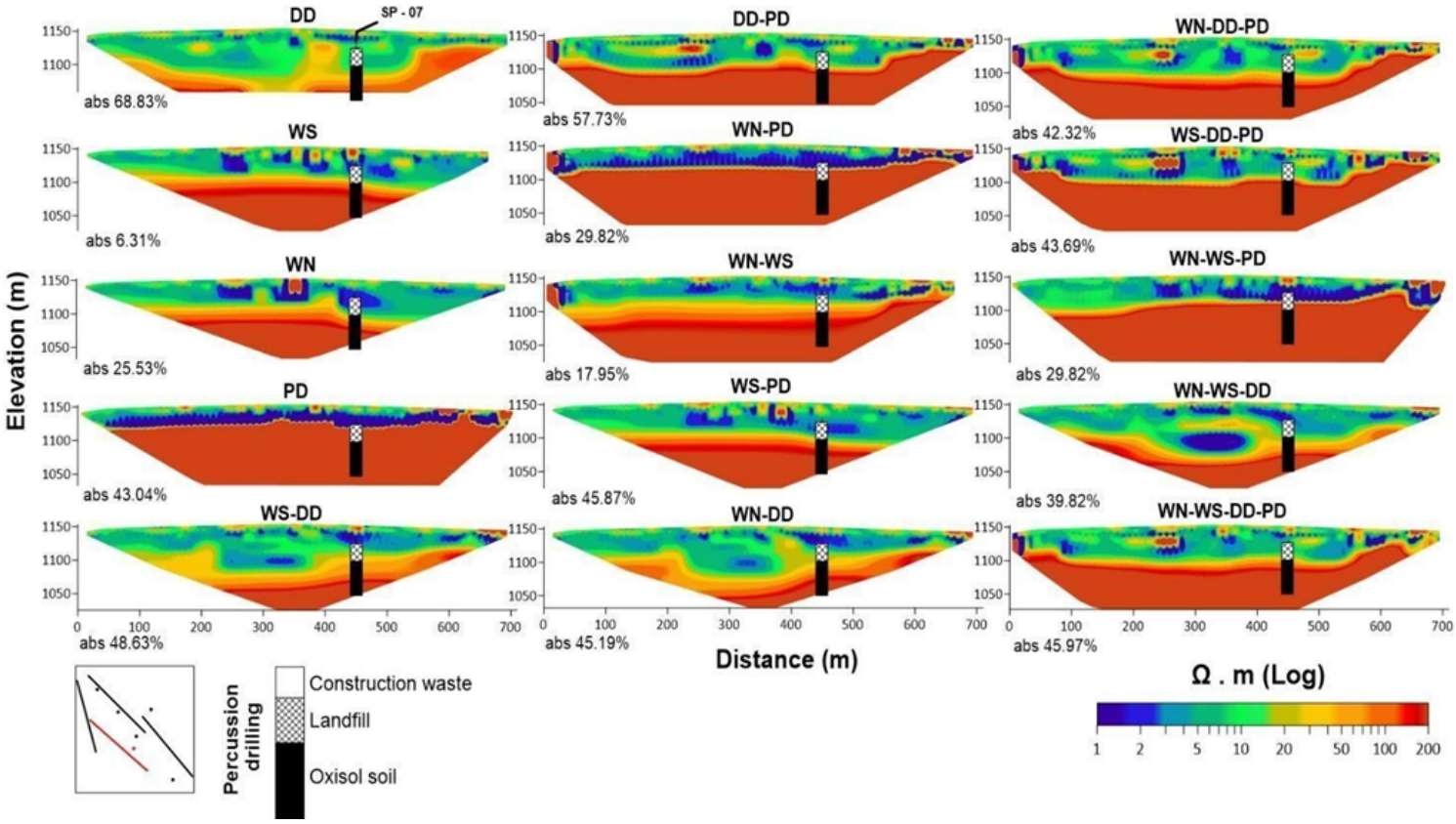

Figure 5

Comparison between resistivity sessions for line 3 obtained for the 4 arrays and 11 inversion combinations, associated with the drillhole SP-07.

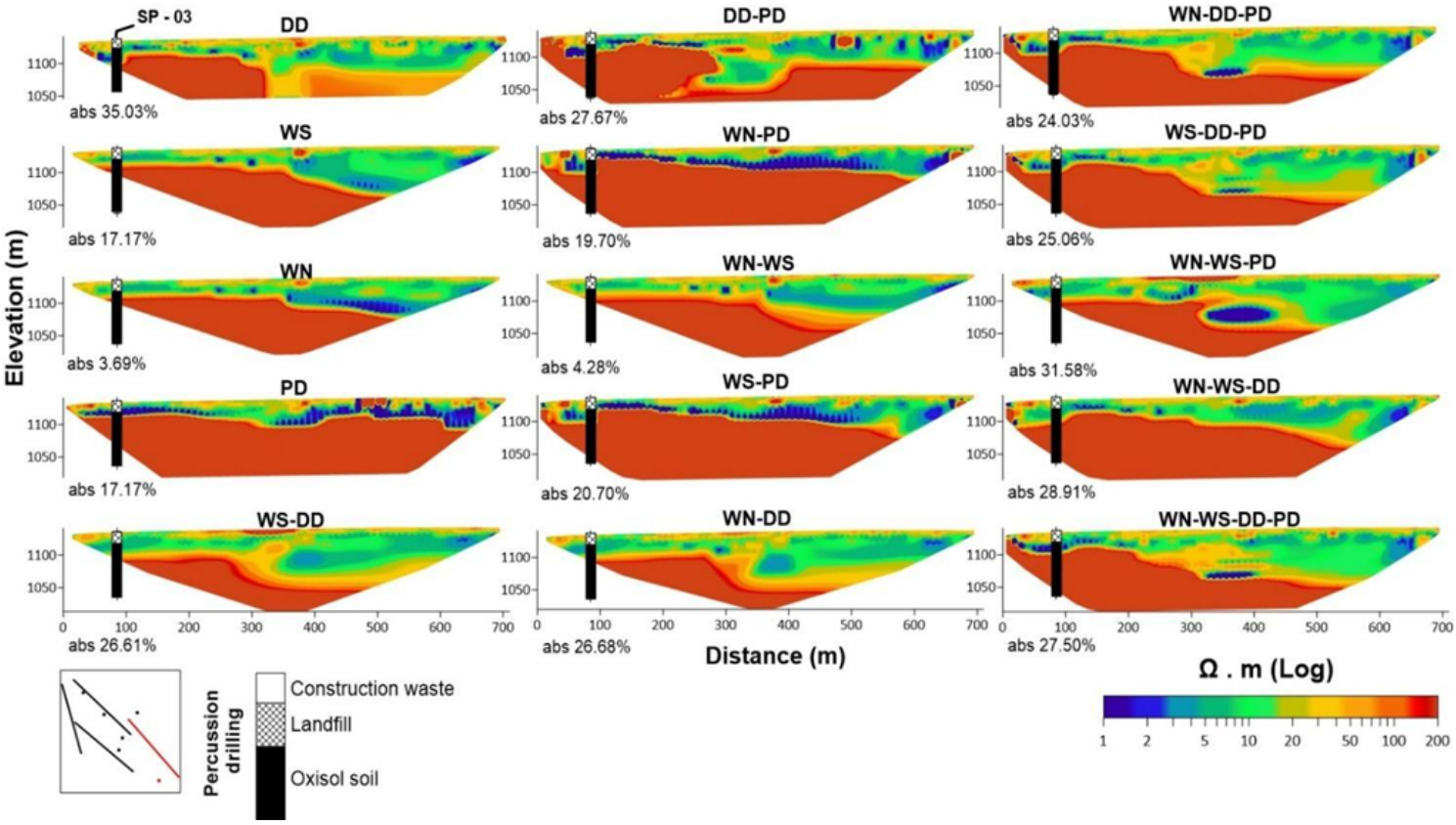

Figure 6

Comparison between resistivity sessions for line 4 obtained for the 4 arrays and 11 inversion combinations, associated with the drilling hole SP-03.

Figure 7

Statistical analysis of the resistivity profiles of the resistivity sessions (1, 2 and 4 and numerical model), along the drillholes (PG1, SP-03, SP-04, SP-07). A) Resistivity profiles by depth along the drillholes, containing the resistivity profile regarding the section of each inverted arrangement combination. B) Values of $\beta 1$ and Range referring to the resistivity values along the drillholes, with an interval of 10 meters from the top and bottom of the waste package. In green, the combinations of arrays with the best results of the statistical parameters are highlighted.

Figure 8

a) Model of ETR from lines 1 to 4 obtained by the simultaneous inversion of the WN-DD configuration with the projection of the geological surveys. The black and gray lines represent the resistivity isovalues used for surface interpolation. The interpolated model of the thickness of the waste package of the investigated area of the ACJC. b) Map of the thickness of the waste layer for the investigated area of the ACJC landfill. c) 3D model of the ACJC waste layer thickness. d) 2D profile of the waste layer (NW-SE) of the investigated area. e) Histogram of error relative to the actual and measured values for the base and top of the waste layer, and the values of RMSE and Pearson's correlation coefficient (φ) calculated f) Semivariogram of the base and top data of the landfill adjusted to the exponential model, as well as the parameters of the theoretical function Sill and Range used.